THE MOVEMENT AND SHAPE CHANGE CHARACTERISTICS OF A BUBBLE PASSING THROUGH A LIQUID-LIQUID INTERFACE

by

Jiarui XU[a,b], Xiaohui ZHANG[a,b], Shan QING[a,b], and Jiaying WU[a,b]*

[a] Faculty of Metallurgical and Energy Engineering, Kunming University of Science and Technology, Kunming, China
[b] National Local Joint Engineering Research Center of Energy Saving and Environmental Protection Technology in Metallurgy and Chemical Engineering Industry, Kunming University of Science and Technology, Kunming, China

In order to study the movement and shape change characteristic of bubble when passing through the interface of two kinds of liquids with different viscosity, the free rising process of a single bubble in static stratified liquids was numerically simulated with the volume-of-fluid method. The results show that, when the initial height of bubble rising is the same, the rising velocity, deformation increase with the increase of bubble radius. When the maximum intensity of the vortex in the bubble is distributed at the top of the bubble, the top of the left and right sides and the bottom of the left and right sides, the bubble shape is spherical, ellipsoid and spherical cap shape respectively. At different initial heights, the bubble trajectory shows three different shapes – linear, spiral, and C-shaped. The relationship between the bubble aspect ratio and rising height is predicted when different radius bubble passing through the interface. The amount of liquid B (lower layer) carried by the bubble increases with the increase of the bubble's initial radius, and the amount of liquid carried by bubbles in C-shaped trajectory is higher than that in spiral trajectory.

Key words: *multiphase flow, single bubble, shape analysis, immiscible fluids,
rising behavior*

Introduction

The bubble movement in two immiscible liquids is a typical multiphase flow phenomenon during metal melting [1]. In multiphase flow system, the generation of air bubbles and the movement process are affected by a variety of forces, such as buoyancy, resistance, surface tension, *etc.*, which have an important impact on the gas-liquid phase. When bubbles move in two immiscible fluids, the movement of bubbles becomes more complex and unstable due to the difference of density and viscosity between the two liquids.

Numerical simulation methods of bubble motion have been extensively studied by many researchers, such as volume-of-fluid (VOF) method [2, 3], level set method [4], lattice Boltzmann method [5], smooth particle hydrodynamics (SPH) method [6], an improved numerical algorithm for front tracking method [7], and moving particle semi-implicit (MPS) method [8], *etc.* The rising trajectory of a single bubble is related to the fluid properties. In the

---

high viscosity liquid, the bubble rises steadily along a straight line. In the medium viscosity liquid, it rises first along a straight line, then becomes a zigzag rise. In the low viscosity liquid, the bubble rises in a spiral way, accompanied by violent swing and rotation [9]. For the study of bubble shape change, Hua *et al.* [7] used a new front tracking method to predict the shape change of bubbles with different initial radius in viscous liquid. It was found that with the increase of bubble diameter, the bubble deformation was more intense, and the correctness of the prediction was verified by experiments. When the bubble diameter is less than 5.0 mm, the method has good prediction. Hashida *et al.* [10] explored the trajectories of a single bubble in water and glycerin aqueous solution respectively, and discussed the relationship between bubble diameter and bubble trajectories. Li *et al.* [11] explored the deformation rules of single bubble in water and three different densities of glycerine, and found that the smaller the liquid viscosity, the more severe the bubble deformation, and the different distribution of internal vortices of bubbles with different shapes. As early as 1954, Garner *et al.* [12] deduced the rising velocity equations of elliptical and elliptical cap bubbles in the main axis direction. Park *et al.* [13] optimized the method for measuring the bubble rising velocity, and proposed a simple parameterization. Compared with the previous suggested parameterization, it no longer required the prior knowledge of bubble shape to monitor the bubble velocity, and it began to be used as a clear formula. Some researchers [14-16] analyzed the growth rule of bubbles, and verified that the bubble frequency and shape can be controlled by cross flow rate.

In addition, many experts have also studied the movement behavior of bubbles in two immiscible liquids. Szekely [17] proposed a mathematical model to describe the heat and mass transfer mechanism between two immiscible solutions under the action of bubble agitation. Greene *et al.* [18] studied the phenomenon of the amount of liquid carried by bubbles through two immiscible liquids by combining theoretical analysis with experimental verification. Yang *et al.* [19] studied the influence of the deformation process of the top-blown bubbles at the interface of two fluids with different viscosity on the mixing effect. Natsui *et al.* [20-22] used an improved SPH model to study the bubble behavior at the liquid-liquid interface, and the simulation results were similar to those obtained by Kochi *et al.* [23] with VOF method. Travis *et al.* [24] studied the effect of initial bubble diameter on bubble growth rate in immiscible liquids. Dong *et al.* [8] analyzed the mass transfer effect of a single bubble at the interface of two immiscible liquids by MPS method, and found that when the viscosity ratio of the two liquids was 2.5, the lower liquid carried by the bubble to the upper liquid.

Although there are a lot of substantial research on the deformation law and movement characteristics of single bubble, there are few studies on the shape change and rising process of single bubble passing through the interface of two immiscible liquids. Therefore, this paper will study the rising behavior of a single bubble with four different initial radius (2 mm, 3 mm, 4 mm, and 5 mm) and different initial rising positions (10 mm, 15 mm, 20 mm, and 25 mm) in two immiscible liquids, and simulated the movement process of the bubble at the liquid-liquid interface with VOF method.

Numerical method and verification

Governing equations

In this paper, VOF method is used to simulate the computational domain. The VOF is a simulation method to establish two or more incompatible fluids by tracking the volume fraction of fluid in the whole region.

The basic idea of VOF is: C_q is defined as the volume fraction of q phase, $C_q = 0$, representing gas phase; $C_q = 1$, representing liquid phase; $0 < C_q < 1$, represents the gas-liquid interface.

Interface tracing between phases is realized by solving the continuity of the volume fraction of one (or more) phases [25]. For the q phase, the tracing equation is:

$$\frac{1}{\rho_q}\left[\frac{\partial}{\partial t}(C_q\rho_q) + \nabla(C_q\rho_q\mathbf{v}_q) = \sum_{p=1}^{n}(\dot{m}_{pq} - \dot{m}_{qp})\right] \tag{1}$$

where $\dot{m}_{pq}$ represents the mass transfer from p-phase to q-phase and $\dot{m}_{qp}$ is the mass transfer from phase q-phase to p-phase.

The continuous equation is:

$$\nabla\mathbf{u} = 0 \tag{2}$$

The Navier-Stokes equation can be expressed:

$$\frac{\partial(\rho\mathbf{u})}{\partial t} + \nabla(\rho\mathbf{u}\mathbf{u}) = -\nabla p + \nabla[\mu(\nabla\mathbf{u} + \nabla\mathbf{u}^T)] + \sigma\frac{\rho\kappa\mathbf{n}}{\frac{1}{2}(\rho_l + \rho_g)} + \rho g \tag{3}$$

$$\kappa = \nabla\hat{n} \tag{4}$$

where σ is the surface tension, $\mathbf{u}$ − the velocity vector, and $\hat{n} = \mathbf{n}/|\mathbf{n}|$.

Based on the volume fraction, the density and viscosity are:

$$\rho = C_p\rho_l + (1 - C_p)\rho_g \tag{5}$$

$$\mu = C_p\mu_l + (1 - C_p)\mu_g \tag{6}$$

Physical model and grid independence verification

In order to improve the computational efficiency of the grid, the mesh of the main rising path of a bubble is encrypted. Quadrilateral mesh is used throughout the calculation area and the total number of meshes is 171828. The mesh size of the encrypted area is 0.323×0.323 mm and the mesh size of the unencrypted area is 0.625×0.625 mm. Figure 1(a) shows the calculation area division and monitoring point setting during the bubble movement process.

Figure 1(b) is a schematic diagram of the monitoring point in the process of bubble rising. A monitoring point is set at intervals of 20 mm from the initial position of the bubble to leaving the upper layer liquid (liquid A). A monitoring point is set at intervals of 5 mm between the liquid-liquid interface.

It is assumed that the fluid around the bubble is incompressible, because of the low liquid height, and small pressure changes. In this paper, the movement behavior of bubbles passing through the liquid-liquid interface of A and B at room temperature was studied. The physical properties of the two liquids are shown in tab. 1. The dimension of the calculation area is 600 mm ×50 mm, in which the liquid height of the lower layer and the upper layer are 250 mm, respectively. The bubble is set as a positive sphere, and the initial height is at the center of the *x*-axis and 20 mm from the bottom.
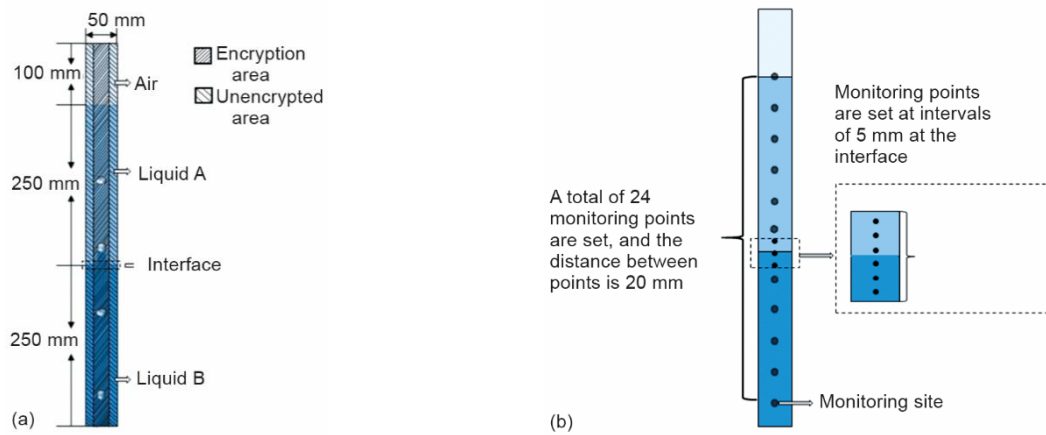
Figure 1. Computational domain diagram; (a) grid division and (b) monitoring point setting

Table 1. Two physical parameters of liquid phase

	ρ [kgm^{-3}]	μ [Pa·s]
Liquid A	800	0.003
Liquid B	1000	0.00103

In this paper, unsteady implicit pressure solver and PISO algorithm [26] are used to couple pressure and velocity. In order to ensure accurate calculation results and reduce calculation costs, grid independence test is necessary. Figure 2 shows the simulation results of aspect ratio and velocity of bubbles of the same radius under five different gird numbers. It can be seen that the bubble aspect ratio of grids A and B is smaller than that of the other three grids before and after crossing the interface, and the bubble rising velocity of grids A and B is quite different from that of grids C, D, and E. However, with the increase of grid number,
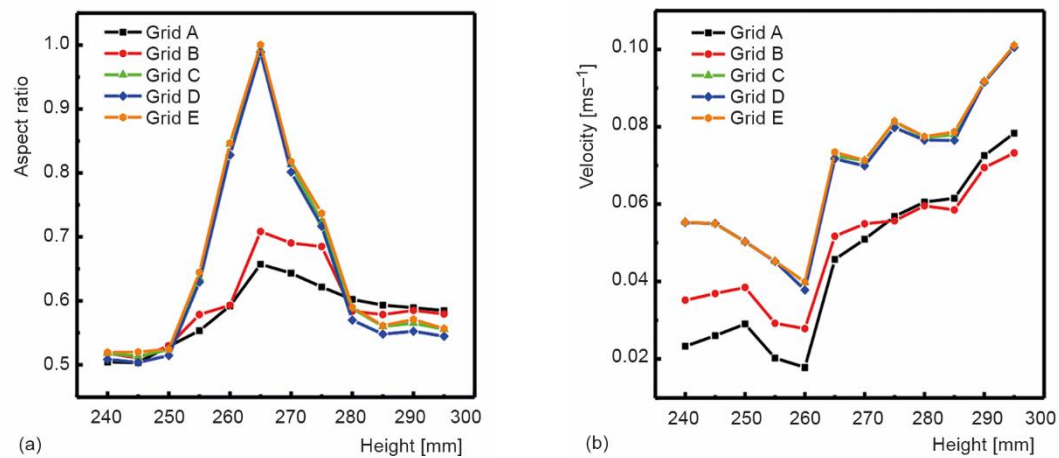

Figure 2. Aspect ratio and velocity of bubble under different mesh conditions;
(a) aspect ratio and (b) velocity

there is no significant change in aspect ratio and rising velocity. Therefore, in order to ensure good calculation results and low calculation cost, grid C condition is selected. Table 2 is the comparison of five grid dimensions.

Table 2. Dimensions of the five gird schemes

Schemes	Total gird number	Number of grid in the encryption area	Number of grid in the unencrypted area
Gird A	24059	12857	11202
Gird B	78392	41829	36563
Gird C	171828	92907	78921
Gird D	301938	161321	140617
Gird E	819384	421675	397709

Model validation

Yang's experimental conditions are shown in tab. 3. In addition, the equivalent diameter of the initial bubble is 5 mm. The simulation conditions are set according to Yang's experimental conditions. The initial radius of the bubble is 2.5 mm. In order to save the calculation cost, the fluid height of the upper and lower layers is set to 250 mm.

Table 3. Yang's experimental conditions [19]

Fluid	Density [kgm^{-3}]	Viscosity [Pa·s]	Liquid height [cm]
Lower layer	1001.00	1.05×10^{-3}	3
Upper layer	916.25	7.13×10^{-3}	3

As shown in fig. 3. Yang's experimental results are on the left and numerical simulation results are on the right. Through results of the simulation and Yang's experiment, the bubble shapes in the initial position, in the lower liquid, between the liquid-liquid interface and about to leave the interface were compared. It was found that the experimental and simulation results were in good agreement.
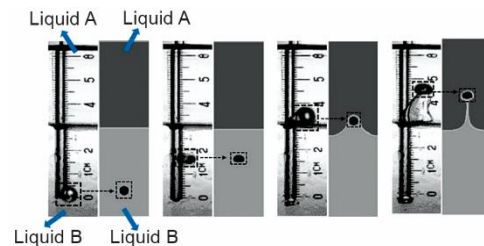

Figure 3. Comparison between simulation results and experimental results of Yang [19]

Results and discussion

The effect of different initial radius

The velocity changes of the bubble are shown in fig. 4. When the bubble first rises from the lower liquid, that is, from the liquid B, the rising velocity of the bubble increases. As the bubble radius increases, its rising velocity also increases slightly, as shown in fig. 4(a). When the bubble rises to the interface, the rising velocity of the bubble decreases, as shown in fig. 4(b). When the bubble passes through the interface and completely separates from liquid B, the rising velocity of the bubble begins to increase.
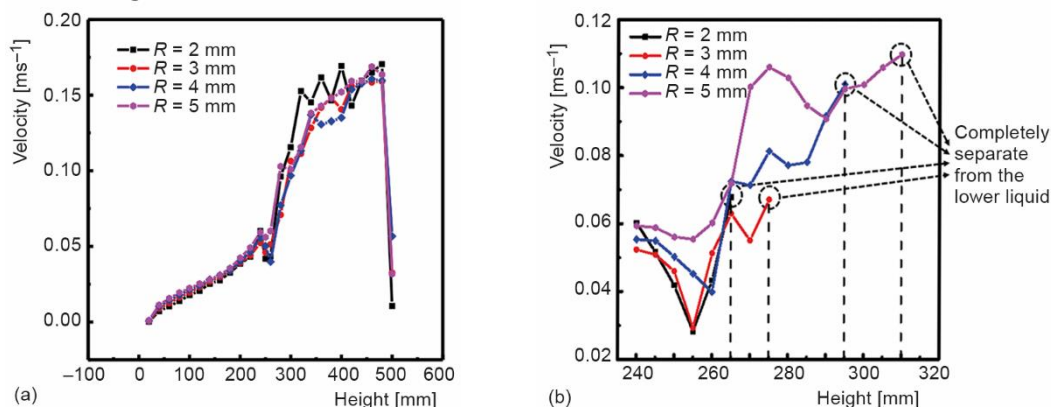
212

Xu, J., *et al.*: The Movement and Shape Change Characteristics of …
THERMAL SCIENCE: Year 2023, Vol. 27, No. 1A, pp. 207-217

Figure 4. The velocity changes during bubble rising with different radius; (a) from liquid B to leaving liquid A and (b) during the interface

Figure 5 shows the shape change of bubble rising process. During the rising process of liquid B, the bubble gradually changes from the initial original sphere to the ellipsoid. With the increase of bubble radius, the deformation trend of bubble is more obvious. When the bubble passes through the interface, the bubble changes from ellipsoid to regular sphere. As the bubble continues to rise, its shape gradually changes from spherical to ellipsoid and cap.

As shown in fig. 6, the trajectory of bubble rising process is presented. The coordinates of the center of mass in the rising process of the bubble are obtained. Figure 6 shows the trajectories of four bubbles with different radius in two immiscible liquids A and B. It can be seen that the bubble rises approximately in a straight line in the liquid B, and after passing through the interface, the bubble rises in C-shape. The smaller the bubble radius is, the more the trajectory deviates from the central axis. With the increase of the bubble radius, the end point of the bubble motion is closer to the vertical direction of the bubble starting point, until the coincidence.
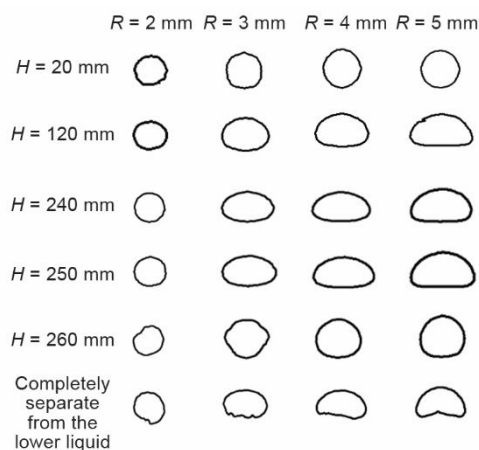

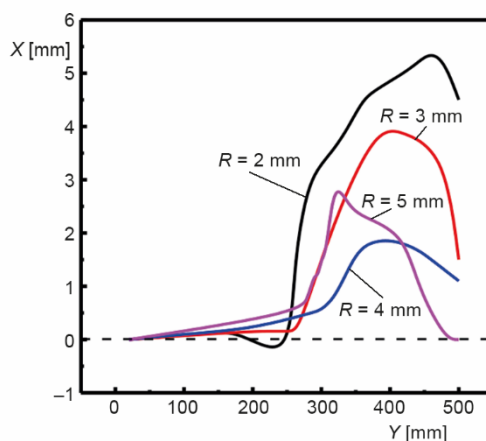**Figure 5. Outline of bubble passing through interface (different radius, same initial height)**

Figure 6. Trajectory of bubbles with different radius

The vortex intensity change of the bubble when it passes through the interface is shown in fig. 7. The vortex intensity in the bubble is closely related to the change of bubble shape in the rising process. The circulation inside the bubble is caused by the change of the viscosity of the external fluid and the viscosity resistance [12].

Figure 7. Distribution of vortex intensity in bubbles with different initial radius

Taking the bubble with a radius of 4 mm as an example, when the bubble has not yet touched the interface, that is, the rising height of the bubble is 240 mm, the position of the maximum vortex intensity is symmetrically distributed on the left and right sides of the bubble. When the bubble rises to 250 mm, the position of the maximum vortex intensity is still distributed on the left and right sides of the bubble. When it rises to 260 mm, that is, when the bubble reaches the interface, the bubble changes from ellipsoid to sphere. At this time, the position of the maximum vortex intensity is distributed on the top of the bubble. When the bubble continues to rise until it completely separated from the lower liquid, the bubble changes from a spherical shape to an ellipsoid shape. At this time, the position of the maximum vortex intensity is distributed on the two sides below the bubble. As the bubble rises, the intensity of vortex also increases.
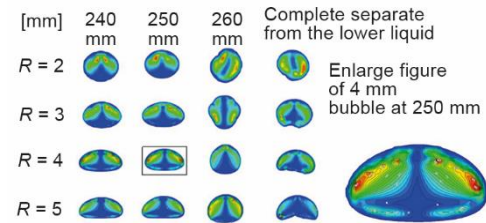
The effect of different initial height

Figure 8 shows the rising trajectory of bubbles with a radius of 4 mm at different initial heights. In order to study the influence of different pressure and initial velocity on the bubble rising process, the initial bubble height is set to 10 mm, 15 mm, 20 mm, and 25 mm. When the initial height is 10 mm, the bubble rises approximately in a straight line in liquid B, and after passing through the interface, it rises in a C-shape. When the initial height is 15 mm, it rises in a C-shape in liquid B, and then rises in a spiral shape after crossing the interface. When the initial height is 20 mm, the bubble rises in a straight line with a slope of about 30° in liquid B. After passing through the interface, it rises in a C-shape. When the initial height is 25 mm, it

Figure 8. Bubble trajectories at different initial height

rises in a C-shape in liquid B, and after passing through the interface, it rises in a spiral shape. Bubbles with different initial heights have different pressures, resulting in different bubble trajectories.
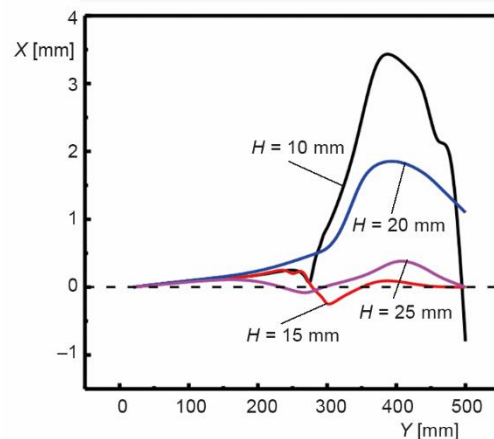
Figure 9 shows the distribution of vortex intensity inside the bubble at the initial height. It can be seen that the vortex intensity increases with the rise of the bubble. Before the bubble completely separates from the lower liquid, there is no significant difference in its shape and internal vortex intensity distribution. When the bubble completely separates from the lower liquid, that is to say, when it reaches the height of 295 mm, there is an obvious
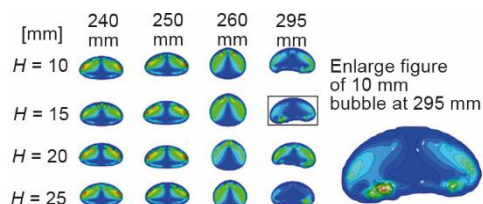
214

Xu, J., *et al.*: The Movement and Shape Change Characteristics of …
THERMAL SCIENCE: Year 2023, Vol. 27, No. 1A, pp. 207-217

Figure 9. Distribution of vortex intensity in bubbles at different initial heights

change in the bubble shape. At this time, the greater vortex intensity in the bubble is mainly distributed on left and right sides of bubble's bottom. However, the maximum of vortex intensity is different in different initial heights. When the bubble with the initial height of 25 mm is completely separated from the lower liquid, the vortex intensity inside the bubble is less than the other three initial heights, but the distribution of its maximum value is similar to that of the other three, which are mainly distributed on the bottom of the bubble. As an example, when the initial height of the bubble is 15 mm and the height is 295 mm, it can be seen that the left lower part of the bubble is more prominent than the right lower part, and the maximum vortex intensity in the bubble is mainly distributed in the lower left part of the bubble.

Law of bubble shape change

In order to quantify the change of bubble shape more clearly, the bubble aspect ratio, *Ar*, is calculated.

$$Ar = \frac{D_x}{D_y} \tag{7}$$

where D_x is the length in the horizontal direction and D_y is the length in the vertical direction.

As shown in fig. 10, it is the relationship between the aspect ratio of bubbles and the height of liquid carried. The aspect ratio of bubbles is related to the radius and the rising height of bubbles when passing through the interface. Therefore, fitting the correlation formula of these parameters is helpful to predict the shape variables of bubbles with different sizes.
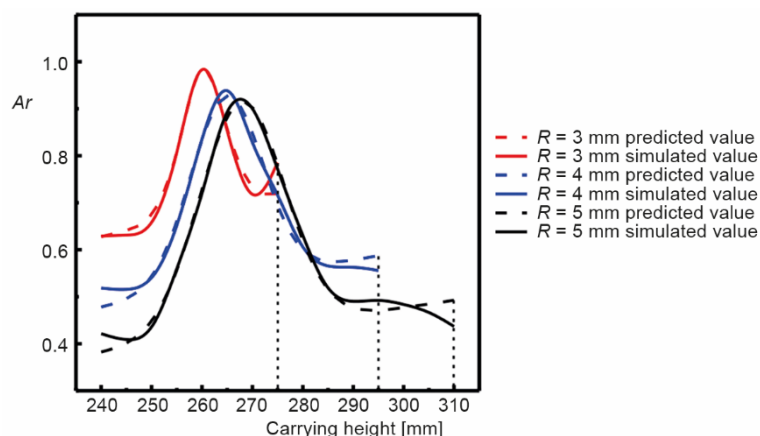

Figure 10. Comparison of predicted value and simulated value of correlation between aspect ratio and carrying height

The relationship between the carrying height and aspect ratio with three different radii when passing through interface is summarized as follows:

− for R = 3 mm:

$$y = 0.002616x + 0.390456 \times 0.218068^{\frac{(x-260.288743)^2}{2 \times 2.621541^{2.955769}}}$$

(8)

− for R = 4 mm:

$$y = 0.001991x + 0.437844 \times 0.884292^{\frac{(x-264.9088)^2}{2 \times 1.28407^{6.630365}}}$$

(9)

− for R = 5 mm:

$$y = 0.001589x + 0.0.520424 \times 0.893237^{\frac{(x-267.919593)^2}{2 \times 1.503101^{4.808867}}}$$

(10)

where x represents the carrying height of bubble and y the aspect ratio.

The bubble shape changes with the transfer of the concentration region of the maximum vortex intensity. The maximum value of bubble aspect ratio increases with bubble radius. Because the larger the bubble radius is, the greater the resistance is, the slower the shape recovery is.

Conclusions

In this paper, the VOF method is used to simulate the movement of a single bubble when passing through the liquid-liquid interface. It is found that the liquid properties and the bubble initial radius have a great influence on the shape change and movement characteristics of the bubble during the rising process. The following conclusions are obtained:

- When a bubble rises in a less viscous liquid, its shape gradually changes from spherical to ellipsoidal, while in a more viscous liquid, its shape changes from spherical to ellipsoidal, and then to spherical cap. With the increase of bubble radius, the deformation becomes more intense.
- When the bubbles passing through the interface, the shape of the ellipsoid will gradually return to the sphere. After passing through the interface completely, the bubble done a complete process of bubble rising deformation, that is, its shape changes from sphere to ellipsoid, and then to spherical cap. In the whole process of rising movement, the bubble velocity first increases, then decreases and then increases.
- The change of bubble shape can be judged by the distribution of vortex intensity inside the bubble. When the position of the maximum vortex intensity is mainly at the top of the bubble, the bubble is nearly spherical, when the position of the maximum vortex intensity is distributed on the left and right sides of the bubble, the bubble is elliptical, and when the position of the maximum vortex intensity is mainly concentrated at the lower left and right sides of the bubble, the bubble is in the shape of a spherical cap.
- The mathematical relation between bubble aspect ratio and carrying height is obtained by fitting.
- The amount of liquid carried increases with the increase of the bubble radius. The bubble rises from different initial heights, the bubble trajectory is different, and the position of the maximum intensity of the vortex in the bubble is also different.

216

Xu, J., *et al.*: The Movement and Shape Change Characteristics of …
THERMAL SCIENCE: Year 2023, Vol. 27, No. 1A, pp. 207-217

Acknowledgement

Nomenclature

Ar – aspect ratio, [–]
C – volume fraction, [–]
D_x – length in the horizontal direction, [mm]
D_y – length in vertical direction, [mm]
g – gravitational acceleration, [ms^{-2}]
H – initial height, [mm]
p – pressure, [Pa]
R – bubble radius, [mm]
t – time, [s]
v, u – velocity vector, [ms^{-1}]

Greek symbols

ρ – density, [kgm^{-3}]
μ – viscosity, [Pa·s]
σ – surface tension coefficient, [Nm^{-1}]

Subscripts

p, q, g, l – phase

References

[1] Liu, Y., *et al.*, A Review of Physical and Numerical Approaches for the Study of Gas Stirring in Ladle Metallurgy, *Metall. Mater. Trans. B., 50* (2019), Nov., pp. 555-577
[2] Li, T., *et al.*, Numerical Investigation of an Underwater Explosion Bubble Based on FVM and VOF, *Appl. Ocean Res., 74* (2018), 1, pp. 49-58
[3] Abbassi, W., *et al.*, Study of the Rise of a Single/Multiple Bubbles in Quiescent Liquids Using the VOF Method, *J. Braz. Soc. Mech. Sci. Eng., 41* (2019), 6, pp. 1678-5878
[4] Grave, M., *et al.* A New Convected Level-Set Method for Gas Bubble Dynamics,*Comput. Fluids, 209* (2020), Sept., 104667
[5] Shu, S., *et al.*, GPU-Accelerated Transient Lattice Boltzmann Simulation of Bubble Column Reactors, *Chem. Eng. Sci., 214* (2020), Mar., 115436
[6] Li, M., *et al.*, An Axisymmetric Multiphase SPH Model for the Simulation of Rising Bubble, *Comput. Methods Appl. Mech. Engrg., 336* (2020), July, 113039
[7] Hua, J., *et al.*, Numerical Simulation of Bubble Rising in Viscous Liquid, *J. Comput. Phys., 222* (2007), 2, pp. 769-795
[8] Dong, C. H., *et al.*, Simulation on Mass Transfer at Immiscible Liquid Interface Entrained by Single Bubble Using Particle Method, *Nucl. Eng. Technol., 52* (2020), 6, pp. 1172-1179
[9] Liu, Z. L., *et al.*, Study of Bubble Induced Flow Structure Using PIV, *Chem. Eng. Sci., 60* (2005) 13, pp. 3537-3552
[10] Hashida, M., *et al.*, Rise Velocities of Single Bubbles in A Narrow Channel Between Parallel Flat Plates, *Int. J. Multiphase Flow., 111* (2019), Feb., pp. 285-293
[11] Li, X. , *et al.*, Analysis of Deformation and Internal Flow Patterns for Rising Single Bubbles in Different Liquids, *Chinese J. Chem. Eng., 27* (2019), 4, pp. 745-758
[12] Garner, F. H., *et al.*, Circulation Inside Gas Bubbles, *Chem. Eng. Sci., 3* (1954), 1, pp. 1-11
[13] Park, S. H., *et al.*, A Simple Parameterization for the Rising Velocity of Bubbles in a Liquid Pool, *Nucl. Eng. Tech., 49* (2017), 4, pp. 692-699
[14] Chen, G., *et al.* Study on the Bubble Growth and Departure with A Lattice Boltzmann Method,*China Ocean Eng., 34* (2020), 1, pp. 69-79
[15] Sepahi, F., *et al.* The Effect of Buoyancy Driven Convection on the Growth and Dissolution of Bubbles on Electrodes, *Electrochim. Acta, 403* (2022), Jan., 139616
[16] Higuera, F. J., A Model of the Growth of Hydrogen Bubbles in the Electrolysis of Water, *J. Fluid Mech., 927* (2021), Sept., A33
[17] Szekely, J., Mathematical Model for Heat or Mass Transfer at the Bubble-Stirred Interface of Two Immiscible Liquids, *Int. J. Heat Mass Transf., 6* (1963), 5, pp. 417-422
[18] Greene, G. A., *et al.*, Onset of Entrainment Between Immiscible Liquid Layers Due to Rising Gas Bubbles, *Int. J. Heat Mass Transf., 31* (1988), 6, pp. 1309-1317

Xu, J., *et al.*: The Movement and Shape Change Characteristics of …
THERMAL SCIENCE: Year 2023, Vol. 27, No. 1A, pp. 207-217

217

[19] Yang, P. Y., *et al.*, Experimental Study on the Influence for Stirring Effect of the Bubbles Deformation Through Two Phases in Top Blowing Bath (in Chinese), *Chem. Ind. Eng. Prog., 33* (2014), 3, pp. 617-622

[20] Natsui, S., *et al.*, SPH Simulations of the Behavior of the Interface Between Two Immiscible Liquid Stirred by the Movement of a Gas Bubble, *Chem. Eng. Sci., 141* (2016), 1, pp. 342-355

[21] Natsui, S., *et al.*, Stable Mesh-Free Moving Particle Semi-Implicit Method for Direct Analysis of Gas-Liquid Two-Phase Flow, *Chem. Eng. Sci., 111* (2014), 1, pp. 286-298

[22] Natsui, S., *et al.*, Multiphase Particle Simulation of Gas Bubble Passing Through Liquid/Liquid Interfaces, *Mater. Trans., 55* (2014), 11, pp. 1707-1715

[23] Kochi, N., *et al.*, Numerical Simulation on Penetration Stage of a Rising Bubble through an Oil/Water Interface, *ISIJ Int., 51* (2011), 6, pp. 1011-1013

[24] Travis, S. E., *et al.*, Bubble Growth Inside an Evaporating Liquid Droplet Introduced in an Immiscible Superheated Liquid, *Int. J. Heat Mass Transf., 127* (2018), Dec., pp. 313-321

[25] Hirt, C. W., *et al.*, Volume of Fluid (VOF) Method for the Dynamics of Free Boundaries, *J. Comput. Phys. 39* (1981), 1, pp. 201-225

[26] Issa, R. I., Solution of the Implicitly Discretised Fluid Flow Equations by Operator-Splitting, *J. Comput. Phys., 62* (1986), 1, pp. 40-65